Calcium channel structural determinants of synaptic transmission between identified invertebrate neurons

Spafford, J.D.; Munno, D.W.; van Nierop, P.; Feng, Z.P.; Jarvis, S.E.; Gallin, W.J.; Smit, A.B.; Zamponi, G.W.; Syed, N.I.

published in
Journal of Biological Chemistry
2003

DOI (link to publisher)
10.1074/jbc.M211076200

document version
Publisher's PDF, also known as Version of record

THE JOURNAL OF BIOLOGICAL CHEMISTRY
Vol. 278, No. 6, Issue of February 7, pp. 4258–4267, 2003
Printed in U.S.A.

Calcium Channel Structural Determinants of Synaptic Transmission between Identified Invertebrate Neurons*

Received for publication, October 29, 2002, and in revised form, November 25, 2002
Published, JBC Papers in Press, November 27, 2002, DOI 10.1074/jbc.M211076200

J. David Spafford‡§¶, David W. Munno§‖, Pim van Nierop‡, Zhong-Ping Feng‡, Scott E. Jarvis§‖, Warren J. Gallin‡‡, August B. Smit‡, Gerald W. Zamponi§ §§, and Naweed I. Syed§¶¶**

From the ‡Department of Molecular and Cellular Neurobiology, Vrije Universiteit, Amsterdam, 108HV Netherlands, the §Departments of Physiology and Biophysics, and Anatomy and Cell Biology, University of Calgary, Calgary T2N 4N1, Canada, and the ‡‡Department of Biological Sciences, University of Alberta, Edmonton T6G 1E9, Canada

We report here that unlike what was suggested for many vertebrate neurons, synaptic transmission in *Lymnaea stagnalis* occurs independent of a physical interaction between presynaptic calcium channels and a functional complement of SNARE proteins. Instead, synaptic transmission in *Lymnaea* requires the expression of a C-terminal splice variant of the *Lymnaea* homolog to mammalian N- and P/Q-type calcium channels. We show that the alternately spliced region physically interacts with the scaffolding proteins Mint1 and CASK, and that synaptic transmission is abolished following RNA interference knockdown of CASK or after the injection of peptide sequences designed to disrupt the calcium channel-Mint1 interactions. Our data suggest that Mint1 and CASK may serve to localize the non-L-type channels at the active zone and that synaptic transmission in invertebrate neurons utilizes a mechanism for optimizing calcium entry, which occurs independently of a physical association between calcium channels and SNARE proteins.

Calcium entry through voltage-gated calcium channels triggers the release of synaptic vesicles in the presynaptic nerve terminal. It is thought that the high calcium buffering capacity of neurons necessitates that the sensor for calcium-triggered exocytosis be situated close to the source of calcium entry, *i.e.* near the inner mouth of presynaptic calcium channels (1–3). Accordingly, a region within the cytoplasmic linker connecting domains II–III of mammalian N- and P/Q-type calcium channels, termed the synaptic protein interaction (*synprint*) site, was shown to bind tightly to a number of different proteins of the presynaptic vesicle release complex, including syntaxin1A, SNAP-25, and synaptotagmin1 (4–6). In mammalian neurons, the requirement for a physical complex between presynaptic calcium channels and the SNARE[1] complex is supported by the observation that injection of peptides corresponding to the *synprint* site blocks synaptic transmission, presumably through a competitive decoupling of the SNARE protein-calcium channel complex (2, 7–8).

The physiology of invertebrate synapses appears to correlate closely with their mammalian counterparts. With few notable exceptions, most vertebrate proteins involved in synaptic transmission have structurally conserved orthologs in invertebrates (9). Surprisingly, however, none of the invertebrate calcium channels identified from *Drosophila* or *Caenorhabditis elegans* (10) appear to carry a structural motif that would resemble *synprint*, indicating that a correlate role of *synprint* does not exist in invertebrates. However, this postulate has not yet been tested directly because invertebrate models that are suitable for genetic analysis of synaptic transmission in the central nervous system (such as *C. elegans* and *Drosophila*) are not amenable to direct physiological analysis at the level of single pre- and postsynaptic neurons. Conversely, most invertebrate model systems that are amenable for physiological analysis, until recently, lacked molecular information that is required to interpret the physiological data.

To determine how transmitter release in invertebrates occurs in the absence of calcium channels with a *synprint* motif, we have taken advantage of identified *Lymnaea* neurons, which are directly accessible to both physiological and molecular analysis at the level of single pre- and postsynaptic neurons. We have identified the sequences of the major calcium channel subunits and key synaptic elements, including SNARE proteins that are expressed in the presynaptic neuron. We provide evidence that synaptic transmission is dependent on a *Lymnaea* homolog of mammalian presynaptic calcium channels that does not associate with the SNARE complex. Yet, despite the lack of a *synprint* region in the *Lymnaea* channel isoform, the injection of mammalian *synprint* peptide into *Lymnaea* synapses still inhibits synaptic transmission. Thus, we challenge the current thinking of an unequivocal role of *synprint* in the molecular assembly of synaptic proteins with calcium channels at the active synaptic zone. Instead, we show that synaptic transmission in *Lymnaea* is critically dependent on the expres-

* This work was supported in part by operating grants from the Canadian Institutes of Health Research (to N. I. S. and G. W. Z.). The costs of publication of this article were defrayed in part by the payment of page charges. This article must therefore be hereby marked "*advertisement*" in accordance with 18 U.S.C. Section 1734 solely to indicate this fact.

¶ Recipient of a postdoctoral fellowship award from the Human Frontiers in Science Program.

‖ Supported by from Alberta Heritage Foundation for Medical Research Studentships.

** Recipient of a Canadian Institutes of Health Research postdoctoral fellowship award.

§§ Recipient of a Senior Scholarship from Alberta Heritage Foundation for Medical Research and is a Canadian Institutes of Health Research Investigator. To whom correspondence should be addressed: Dept. of Physiology and Biophysics, University of Calgary, 3330 Hospital Dr., N. W., Calgary T2N 4N1, Canada. Tel.: 403-220-8687; Fax: 403-210-8106; E-mail: Zamponi@ucalgary.ca.

¶¶ Recipient of a Scientist Award from the Alberta Heritage Foundation for Medical Research and is a Canadian Institutes of Health Research Investigator.

[1] The abbreviations used are: SNARE, soluble NSF attachment protein receptors (where NSF is *N*-ethylmaleimide-sensitive factor); dsRNA, double-stranded RNA; ACh, acetylcholine; qPCR, quantitative, real time PCR; RNAi, RNA interference; HVA, high voltage-activated; LVA, low voltage-activated; VD4, visceral dorsal 4; Bt, Botulinum toxin; EPSP, excitatory postsynaptic potential.

sion of an alternatively spliced C-terminal region of the presynaptic channel homolog that physically and functionally interacts with the scaffolding proteins Mint1 and CASK. Our data suggest that these proteins might be involved in anchoring presynaptic calcium channels at the active zones, thus optimizing calcium entry for transmitter release.

EXPERIMENTAL PROCEDURES

Molecular Cloning and Identification of Lymnaea Orthologs—Parts of novel *Lymnaea* cDNAs were identified by PCR cloning using degenerate primers (see Table I), designed from regions with high sequence identity in aligned protein orthologs described in the GenBank™ data base (NCBI, Bethesda) using cDNA that was synthesized from brain ganglia RNA of adult *Lymnaea stagnalis*.

cDNA clones were isolated by screening of λZAP cDNA libraries of the *Lymnaea* central nervous system. Full-length cDNA clones were generated, using primer walking and 5′- and 3′-rapid amplification of cDNA ends. PCR fragments were amplified with DNA polymerases, Herculase, or Turbo*Pfu* (Stratagene), and final sequences were assembled from at least three independent PCRs. All sequencing was completed in both sense and antisense directions using ABI PRISM 310 Genetic Analyzer (Applied Biosystems, Inc., Foster City, CA).

Conceptual translations were derived from the longest open reading frame. When the protein translation initiation site was uncertain, start sites were inferred from closely related orthologs described in GenBank™. *Lymnaea* orthologs and results of comparison of sequence of putative *Lymnaea* proteins with human orthologs are shown in Table I.

Sequence Alignments—BLASTP retrieved orthologs (GenBank™) of *Lymnaea* proteins were aligned by modified progressive pairwise, multiple alignment in PILEUP (UNIX-based, GCG Wisconsin Package 2002, Accelrys, Madison, WI) and were visually displayed (PLOTSIMILARITY, Accelrys).

Quantitative PCR of Lymnaea Genes in Identified Neurons—Primer pairs for qPCR detection of *Lymnaea* gene transcripts were designed with Primer Express 1.0 software (Applied Biosystems). Each candidate primer pair generated an amplicon of the expected size of 85–120 bp, and PCR efficiencies were tested on *Lymnaea* central nervous system cDNA using serial dilutions of template. Primer dimers were identified by measurable product in the absence of qPCR template. All qPCR primer pairs (see Table I) averaged an amplification efficiency of ~1.9–2.0.

cDNA templates for the qPCR were prepared from single, identified neurons with axons attached by gentle mechanical suction with pulling pipette from each of six *Lymnaea* brain ganglia preparations. cDNA were synthesized as follows: 1) directly from freshly isolated neurons; 2) as unpaired pre- and postsynaptic neurons after 18 h of primary culture on hemolymph-coated coverslips; or 3) as synaptically paired neurons cultured for 18 h (see primary cell culture technique described below for more details).

The freshly isolated and cultured cells were transferred as a collective into a prepared microcentrifuge tube in a minimal volume of culture medium (<3 μl) for immediate total RNA isolation and first strand synthesis, using a protocol as described by Van Kesteren *et al*. (14). For qPCR, primer pairs at 2 pmol each were used in a final PCR volume of 20 μl, using a master-mix of SYBR Green PCR core reagents. The threshold line for determining the value of the cycle of threshold, *Ct*, was set on 0.3 Δ*Rn* (base-line subtracted values) with curves reaching maximally 6–8 Δ*Rn* and base lines of ~0.02 Δ*Rn*. Data were considered only if the Δ*CT* values of control and experimental samples were >8 cycles. The overall cDNA expression levels per sample were normalized to the expression of controls L-aldolase and to L-β-tubulin which both show consistent expression for each cell type, and corresponded proportionally to the different cell diameters.

In Vitro Binding and Yeast Two-hybrid Analyses—Bacterial fusion proteins used in binding assays were constructed by inserting PCR-amplified DNA in-frame into pTRCHis or pRSET (Invitrogen) or pGEX (Amersham Biosciences). Fusion proteins for studying yeast two-hybrid interactions were prepared in-frame with bait LexA DNA binding domain of pHybLex and prey B42 activation domain of pYESTrp2. The following fusion protein constructs for expression were prepared (name, protein residue numbers, vector) as follows: rat Cav2.2 *synprint*: 718–963, pTRCHisC; rat stx1A: 1–268, pGEX-KG; LCa_v2a N terminus: 1–67, pYESTrp2; LCa_v2a I–II linker: 346–509, pYESTrp2, LCa_v2b II–III linker: 714–888, pRSETA. LCa_v2a III–IV linker: 1148–1205, pYESTrp2; LCa_v2a C terminus (CT) CT1: 1596–2141, pRSETC, pGEX4T-1, pYESTrp2; LCa_v2a CT2: 1996–2141, pGEX4T-1, pYESTrp2; LCa_v2a CT3: 1447–1722, pYESTrp2; *Lstx1A*: 1–270, pGEX-4T-1, pHybLex; *LSNAP25:* 1–220, pGEX-4T-1; *LsytI*: 1–418, pGEX-4T-1, *Lmint:* 916–1138, pHybLex; *LCASK*: 576–861, pHybLex.

Detailed methods for the bacterial expression, purification, and *in vitro* binding assay of the fusion proteins have been described previously (11–12). All fusion protein constructs were verified by sequencing and evaluated for measurable expressibility on a size-selected SDS-PAGE gel, using Coomassie Blue protein stain. Preparation of protein extracts of *Lymnaea* brain ganglia and Western blot analysis were performed as described previously (11). *Lymnaea* syntaxin1A was detected by commercial antibody (ANR-002, Alomone Labs, Jerusalem, Israel). For analysis of two-hybrid interactions, yeast bait and prey fusion vectors were transformed into L40 *Saccharomyces cerevisiae* strain, and the binding affinity of the interactions was measured by β-galactosidase activity using *o*-nitrophenyl-β-D-galactoside substrate, qualitatively by filter lift according to manufacturer's instructions (Hybrid Hunter, Invitrogen) and quantitatively in liquid extracts.

Primary Cell Culture—Identified neurons of *L. stagnalis* were isolated and cultured in either a soma-soma configuration or neurite-neurite configuration as described previously (13). In knockdown experiments, identified neurons were initially plated on hemolymph-pretreated glass coverslips (to prevent neuronal adhesion) in conditioned medium bathed in 10 μM antisense/mismatch DNA oligonucleotide probes (14) or 10 μg of dsRNA (for RNA interference) for 3 days. The oligonucleotide or dsRNA-treated neurons were then transferred and paired on poly-L-lysine-pretreated glass coverslips in the presence of CM. In some knockdown experiments, RNAi-treated neurons were tested for non-synaptic release using a "sniffer cell" (15) Transmitter release was detected from a dopamine-releasing cell, RPeD1, using one of its postsynaptic neurons, VK, which displays a depolarizing response to dopamine.

Antisense and RNAi Treatment—15-mer double-stranded DNA antisense calcium channel probes were designed across the start site of LCa_v2: GAACGTGGCCATCCA (95–109), a sequence shared in all *Lymnaea* isoforms identified. Mismatch probes for LCa_v2 consisted of three base changes to the antisense sequence GAAGGTGCCCAACCA. Before treatment to neurons, antisense/mismatch probes were reconstituted in *Lymnaea* saline, passed through a 0.8-μm filter, boiled for 2 min, and cooled on ice.

For RNA interference technique, dsRNA probes were synthesized by the transcription in both sense and antisense strands (MEGASCRIPT; Ambion, Austin, TX) using T7 and T3 promoters in Bluescript II KS^+ vector between base pairs 2237 and 2710 (II–IIII loop LCa_v2a), 2237–2761 (II–III loop LCa_v2b), 6083–6520 (C-terminal LCa_v2a), and 1893–2750 (*LCASK*). RNA probes were resuspended in *Lymnaea* saline, boiled for 2 min, incubated at 65 °C for 15 min, and then allowed to cool to room temperature, enabling single complementary RNA strands to anneal properly. RNA samples were analyzed by agarose gel electrophoresis.

Electrophysiology—Synaptic transmission was monitored by simultaneous intracellular recordings of pre- and postsynaptic neurons using hardware and acquisition/analysis software as described previously (13). Calcium channel activities of VD4 neurons were measured using established whole-cell recording technique (16).

RESULTS

Lymnaea Neurons Express Homologs of Mammalian Calcium Channels and SNARE Proteins—The *Lymnaea* soma-soma synapse is a rapidly emerging model for investigating synaptic function. Until recently, the full potential of this system had not been realized due to lack of genomic information. We have thus used degenerate PCR cloning and screening of *Lymnaea* cDNA libraries of whole brain ganglia to identify orthologs of presynaptic vesicle release proteins and of the pore-forming α_1 subunits of the structural superfamily of voltage-dependent calcium channels. *Lymnaea* calcium channel orthologs include representatives of the major high voltage-activated (HVA) calcium channel classes, L-type (LCa_v1) and non-L-type (LCa_v2), and (LVA) T-type (LCa_v3) channels, as well as a calcium channel β subunit (LCa_vb). In addition, we identified a representative of the functionally unidentified class, dubbed U-type (17). These subunits (four α_1 and one β) are reminiscent of the representation in *Drosophila* and *C. elegans* genomes (10) and likely provide a complete complement of such genes in the *Lymnaea* nervous system.

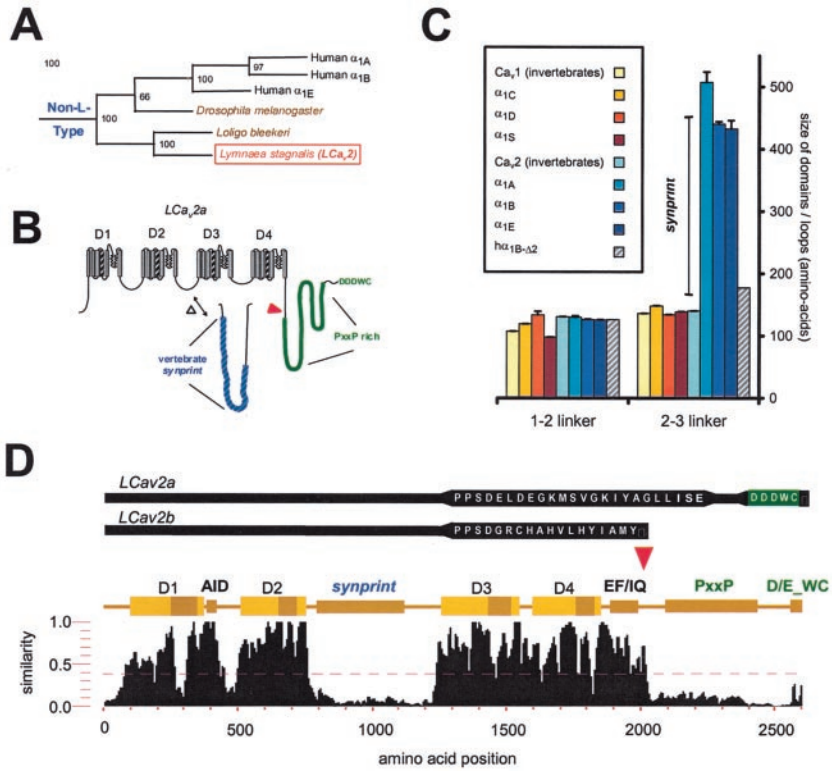

FIG. 1. **Comparison of vertebrate and invertebrate orthologs of Ca_v2 calcium channels.** *A*, phylogram of Ca_v2 α_1 subunits. A single maximum parsimony tree obtained using the heuristic algorithm in PAUP*4.0b8. *Numbers* on the branches are bootstrap support values. *B*, transmembrane topology of the calcium channel α_1 subunit, indicating the absence of the synaptic protein interaction site in invertebrate calcium channels, and the location of proline-rich and DDWC motifs in the C terminus. *C*, region size (mean and S.E.) of the cytoplasmic domain I–II and II–III linkers in Ca_v1 and Ca_v2 representatives from invertebrates (jellyfish, flatworm, nematode, two insects, snail, and squid) and vertebrates (tunicate, fish, marine ray, frog, chicken, rabbit, hamster, mouse, rat, and human) and a human $Ca_v2.2$ splice variant ($\alpha_{1B\text{-}\Delta2}$) lacking the *synprint* site (37). Note that the extended, *synprint*-containing II–III linker region seems exclusive to vertebrate Ca_v2 channels. *D*, similarity between multialigned amino acid sequences of full-length, Ca_v2 calcium channel α_1 subunits from invertebrates (*C. elegans*, *Drosophila*, and *Lymnaea*) and human homologs (α_{1A}, α_{1B}, and α_{1E}). Highlighted with *boxes* are highly conserved regions corresponding to the major transmembrane domains (D1 through D4), and three cytoplasmic regions associated with putatively ascribed binding partners: β subunits (AID), calcium, and calmodulin (EF-hand/IQ motifs) and Mint1 ("(D/E)_WC" motif). The *synprint* region contained in the II–III linker is not conserved among putative full-length Ca_v2 isoforms.

LCa_v2 is a structural homolog of both mammalian N-($Ca_v2.2$) and P/Q-type ($Ca_v2.1$) calcium channels considered responsible for transmitter release at mammalian synapses (18–19), and of invertebrate gene relatives in *Drosophila* (*DmCa1A/cac*) and *C. elegans* (*unc-2*) (20–22) (see Fig. 1*A*). From an alignment of various Ca_v2 homologs (Fig. 1, *C* and *D*), a high degree of sequence conservation is seen in the β subunit interaction site in the domain I–II linker (*AID sequence*) (23) and in the major transmembrane domains, but no apparent sequence identity is evident in the domain II–III linker, the locus of the synaptic protein interaction (*synprint*) site in vertebrate channels (Fig. 1, *C* and *D*). Indeed, the II–III linker region in *LCa_v2* appears considerably shorter than that of vertebrate Ca_v2 channels, and repeated attempts to identify an *LCa_v2* channel with a longer, *synprint*-containing II–III linker in *Lymnaea* cDNA were unsuccessful. In trying to do so, however, we isolated an additional *LCa_v2* isoform (*LCa_v2b*) that varied by 17 amino acids in the II–III linker (see Fig. 1). The apparent lack of the *synprint* motif in *Lymnaea* and other invertebrates contrasts with the high sequence homology among presynaptic vesicle release proteins such as syntaxin1A, SNAP-25, and synaptotagmin1 (see Table I). Taken together, these observations indicate that although SNARE proteins are highly conserved throughout evolution, the appearance of a *synprint* motif may be an evolutionary specialization in vertebrates.

Single-cell Analysis of Transcript Expression in an Identified Presynaptic Neuron—To demonstrate the expression of the identified calcium channel genes, we examined mRNA transcripts in single identified pre- and postsynaptic neurons that are major players in our established soma-soma and neurite-neurite synapse models (13, 24). To ensure unequivocal identification of the cell type, we first acquired an expression profile of cell type-specific markers in three identified neurons as follows: visceral dorsal 4 (VD4), left pedal dorsal 1 (LPeD1), and right pedal dorsal 1 (RPeD1) which form a critical component of a central respiratory rhythm-generating network. Cells were individually isolated from the intact ganglia and subjected to quantitative, real time PCR (qPCR) analysis. For cholinergic/peptidergic presynaptic VD4 neurons, we detected characteristically high *LVAchT* (vesicular acetylcholine transporter) and *LFMRFamide* heptapeptide gene expression levels (Fig. 2). In contrast, the postsynaptic serotonergic neuron (LPeD1) and giant dopamine cell (RPeD1) typically display the higher expression levels of *LVMAT*, the vesicular transporter for monoamines (Fig. 2, *inset*). We then performed real time qPCR in the presynaptic VD4 neuron, using specific primers for the three major types of voltage-gated calcium channels. As seen in Fig. 2, all types of calcium channel α_1 subunits, as well as the β subunit were present in measurable abundance in VD4, including the two C-terminal splice variants of both the *LCa_v1* and *LCa_v2* channels (Fig. 2). In addition, expression of a number of key synaptic proteins such as VAMP, syntaxin1A, SNAP-25, synaptotagmin1, and nsec1/munc18–1 was also detected (not shown, but see Fig. 7*D*). Hence, *Lymnaea* VD4 neurons robustly express many of the proteins thought to be

TABLE I
Molecular cloning, identification, and primer pair sets for Lymnaea genes

Lymnaea gene name	*Lymnaea* GenBank™ gi:	Size of cDNA	Closest human protein gi:	*Vs.* human % similarity/ % identity		Degenerate primer pairs for PCR cloning of *Lymnaea* orthologs	Primer pairs for real time quantitative PCR detection
		bp					
LCa_v1a	AF484079	7391	4502527	62.2	55.2	ATYACMTTYCARGARCARGGNGACCRAAWACYTGC-ATNCCDAT	C terminus, GCATGTGGTTAGCACCTGAGACAGCAATCCCAACAATTATTTCA
LCa_v1b	AF484080	7097	4502527			ATIACIATGGARGGITGGACCCCICCRAAIARYTGCAT	C terminus, GCCAAGAGGTGAGCCAAAGTGACCAGTGCCTGATGCTG
LCa_v1c	AF484081	1701	4502527				
LCa_v2a	AF484082	8239	13386500	62.0	54.7	ATIACIATGGARGGITGGACCCICCRAAIARYTGCAT	C terminus, GCCATACAGCGTTGCAAGAGTTCAACACCAGTCATCGTCATCT
LCa_v2b	AF484083	5603	13386500			ATSGGNATGCARGTNTTYGGTCCTGCCARGCYTCNC-CNGTNGC	C terminus, GATGCCGCCCAGTGATGTCATTCGAGTCACTCTAACAGCAGA I–I linker, TGGGATCGTTCTTCATGCTAAATCTGCGGTTTTCTACCCTTTCT II–III linker, TTTGCCGCTCAAGGGAGACCGGTGATGGAGGACAAATGTT
LCa_v3	AF484084	8350[a]	21361077	55.3	47.0	GTBGTBGARAAYTTYCAYAARTGGYRTCYTTCATDAT-NCCRTTCCA	CCCAGTTGTGCCATCATTACCAGGTGAGGTCTGGACAATGGA
LCa_v4	AF484085 AF484086	6250[a]	3800830	65.3	55.8	GTSTTYHTSGGNTGYATGATHGGTGCATDATNTYRTT-CCARTCYTCNCC	TGTTTGATTCCATCCTTCACTACAGCACCTTGTTCCTTCCACCATAAG
$LCa_v\beta_1$	AF484087	1950	19923119	69.4	61.8	GTSACMGAYATGATGCARAARATGCRTCYTCWARYTG-RKTYTCRTC	CACCATGACGATGACTACGACAGTTCGGAGAAGTGTGGCTGTGA
Lstx1A	AF484088	1278	2501084	80.2	73.3	AARGARGARYTNGARGARYTNATGCATNGCCATRTCC-ATRAACATRTC	AAAACGACAATTGGCCATAACTG TGATTATCCCTTGAGTGAAGATTGC
LSNAP25	AF484089	1811	18765733	64.4	50.7	ATGYTSGACGANCARGGNGARCACATYTCGTCYTCNC-KNGCRTCRTT	ACGTTCGTGTGGATGAAGCA ATCTTCATGGCCCGATCACT
Lsyt1	AF484090	1933	5032139	70.8	62.5	AARAAYYTNAARAARATGGAYGTARNGTRTGCCAYTGN-GCDATNGG	GCGTTCTCGGCTGCAACT CTGTAGTGTGTGCCACTGTGCTAT
$Lsyb_1$	AF484091	784	9257251	72.4	62.9	TTYAARGTSAARACNACNGCNCCACATSKRCTGNACCA-TRAAYTTRTG	GCTGGTGCATCACAGTTTGAA TGCCAATGATAGCTCCCAAGA
LnSec1	AF484092	2099	4507297	73.8	66.3	AARYTSGAYGCNTAYAARGCNGAYGAYTTRTYYTTRTG-CCARTGNCCRTA	GGTGTGACCTACTCTGAAATGAGATG AATGTGGGTCGCACCTATGAG
LVAchT	AF484093	2327	4506991	60.2	51.0	GAYAAYATGYTNTAYATGGTNATHGTGTRTCDATSARD-GCDATNCCRAARCA	CGAACTGTGAGATTGGTTTGATG TCACCCTCTGTTGTTTCCATAACTT
LVMAT	AF484094	2100	4506989	66.1	57.6	ATGGGNATYGCHYTSGGNGGNYTNGCCARAANGCNRC-RTCNGCDATNGCRTA	CACCAGCGAAGGAAGAGAAAAT GGGCTCTTGTCATTCTGATTGTATG
$LMINT_1$	AF484095	4552	22035550	48.4	40.0	AARYTSAAYATHGGNGAYCARATGGCATNGTYTTCATR-TGDATYTC	TTGTCACCCTATTGGCCAGTT TGGAACATCCTGACCAGTTAGAAG
$LCASK_1$	AF484096	3001	4502567	75.8	67.9	ATHATGCAYGGNGGNATGATHCACYTGCCACCARTKRT-GRTCRTCYTT	TTTTTATTGCAGCACCCACACT GTAGGCCTTTTCCAGCAGCTT
L-Aldolase	1730326	1450[a]	4557305	84.7	77.6		TGGCGGTCAATCTGAAGAAGA GAGCTCGGCCATATGAGAATGT
L-β-Tubulin	9625	1709	4507729	95.5	93.7		AGGCGGAATCCAACATGAAC CCCCTCAGCTTCTTCCTCATC

[a] Estimate based on expected size.

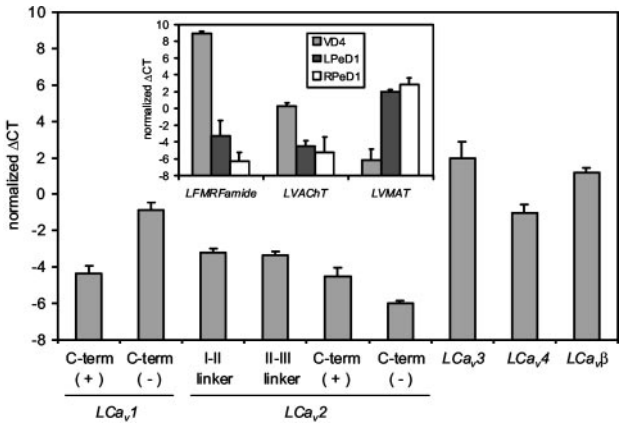

FIG. 2. **Quantification of calcium channel mRNAs in VD4 neurons.** Gene expression measurements using real time qPCR of cDNA synthesized from mRNA of identified neurons freshly isolated from six *Lymnaea* central nerve ring ganglia (mean ± S.E., $n = 6$). Data are represented as the cycle threshold of detection (*CT*), normalized to the expression of control marker gene, L-*aldolase*. *Main panel*, expression profile of calcium channel α_1 subunits (*LCa$_v$1 to Ca$_v$4*) and β subunit in VD4. For both *LCa$_v$1 to LCa$_v$2*, both the full-length, *a* isoform (*C-term* +) and C-terminally truncated *b* isoforms (*C-term* −) are detected. *Inset*, expression profile of cell type-specific marker genes in identified VD4, LPeD1, and RPeD1 neurons. For presynaptic VD4 neurons, the cholinergic/peptidergic neuron phenotype in each sample is confirmed (*i.e.* high *LVAchT* and *LFMRFamide* heptapeptide gene expression). The postsynaptic serotonergic neuron (*LPeD1*) and giant dopamine cell (*RPeD1*) shows the expected serotonin/dopamine phenotype (*i.e.* high levels of *LVMAT*).

involved in mammalian synaptic transmission.

To minimize the possibility that an unidentified *LCa$_v$2* domain II–III linker splice isoform with a *synprint*-like motif could exist in *Lymnaea* neurons, we examined the relative abundance of the *LCa$_v$2* II–III linkers relative to the domain I–II linker region of *LCa$_v$2* which is highly conserved (23) and, thus, a measure of the overall levels of *LCa$_v$2* transcript. As seen in Fig. 2, when we used primers that specifically detected common sequences in both *LCa$_v$2a* and *LCa$_v$2b* but did not produce any gel bands of longer sizes (not shown), we found that the expression of the short II–III linker was strikingly similar to that of the I–II linker. These data suggest that the identified short II–III linkers of *LCa$_v$2a* and *LCa$_v$2b* predominate in VD4, and if an isoform of *LCa$_v$2* with an identifiable *synprint*-containing domain II–III loop were to exist, it can only be of low and almost immeasurable abundance.

Gene Knockdown of Lymnaea Presynaptic Calcium Channels Perturbs Synaptic Transmission—To assess the role of *LCa$_v$2* channels in neurotransmitter release, the presynaptic cell VD4 was pre-treated with antisense and subsequently paired with its postsynaptic partner LPeD1. Specifically, antisense (15-mer) probes were designed at the start site of *LCa$_v$2* channels, and presynaptic VD4 neurons were pre-incubated at a concentration of 10 μM for 3 days before synaptic pairing with postsynaptic LPeD1 neuron. Synapses were subsequently tested with simultaneous intracellular recordings. Unlike control conditions, or in cells injected with mismatch antisense probes (Fig. 3*A*, $n = 12$), excitatory synaptic transmission was perturbed between the soma-soma paired cells (Fig. 3*A*, $n = 9$) in which VD4 cells were selectively treated with antisense-*LCa$_v$2* prior to pairing with LPeD1. Under these experimental conditions, the postsynaptic LPeD1 cells, however, continued to exhibit an excitatory response to exogenously applied ACh, suggesting that the antisense treatment did not affect the postsynaptic cell (Fig. 3*A*). Pre-treatment of VD4 with *LCa$_v$1*-antisense had only a minor effect on synaptic transmission that appeared as a fatiguing of the postsynaptic response over time (not shown).

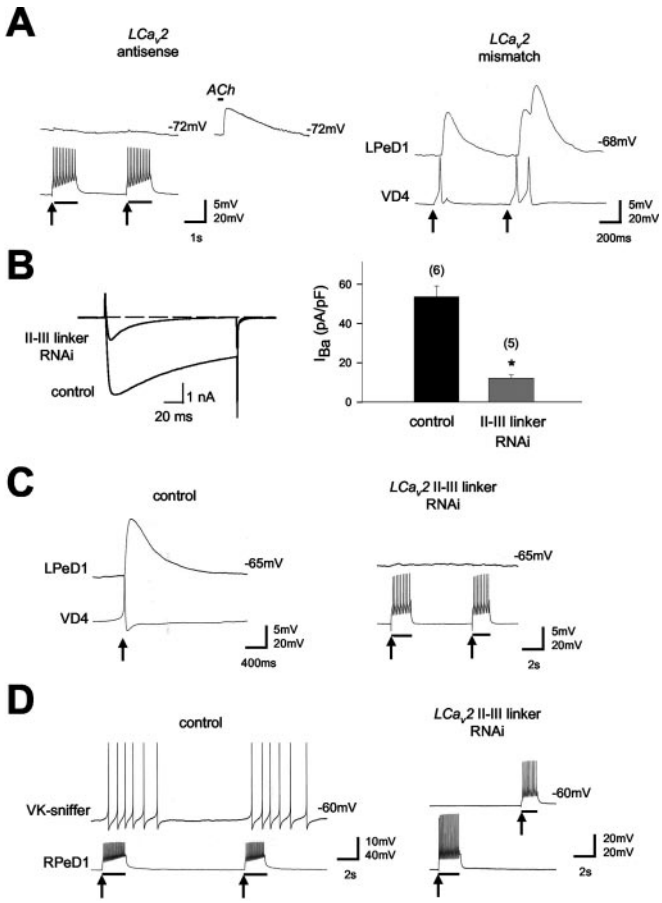

FIG. 3. **Transmitter release requires the *LCa$_v$2* channel.** *A*, isolated VD4 and LPeD1 neurons were treated with 10 μM, 15-mer antisense, or mismatch oligonucleotide probes directed against the start site of *LCa$_v$2*. In pairs treated with antisense probes ($n = 9$), trains of action potentials induced in VD4 (*arrow*) failed to evoke a postsynaptic response in LPeD1. In pairs treated with mismatch probes ($n = 12$), however, action potentials in VD4 (*arrow*) elicit 1:1 EPSPs in the postsynaptic LPeD1 neuron. *LCa$_v$2* knockdown does not affect the postsynaptic cell, which is still responsive to exogenously applied ACh. *B*, RNAi knockdown of the *LCa$_v$2* gene in VD4 reduces the HVA barium current densities, revealing altered kinetics of the remaining currents. Sample recordings display representative currents for both control ($n = 6$) and RNAi ($n = 5$)-treated cells. *C*, knockdown of the *LCa$_v$2* gene via RNA interference. When the pre- and postsynaptic neurons were treated with 10 μg of RNAi directed against the II–III linker of *LCa$_v$2*, synaptic transmission was perturbed ($n = 7$). Induced trains of action potentials in VD4 (*arrow*) fail to elicit a postsynaptic response in LPeD1. In contrast, under control conditions, induced action potentials in VD4 (*arrow*) elicit 1:1 EPSPs in LPeD1. *D*, knockdown of the *LCa$_v$2* gene with RNAi perturbs nonsynaptic release of transmitter. Transmitter release from the dopamine releasing cell RPeD1 ($n = 13$) was detected using a sniffer cell, VK, that depolarizes in response to dopamine. Unlike control cells ($n = 9$), in RNAi treated cells, trains of action potentials in RPeD1 (*arrow*) fail to elicit a response in the sniffer cell VK.

To complement the antisense experiments, we utilized RNA interference (RNAi) techniques to degrade catalytically mRNA in VD4 prior to its pairing with LPeD1. Double-stranded RNA probes were designed against the short II–III linkers found in both *LCa$_v$2a* and *LCa$_v$2b*. VD4 was incubated for 3 days prior to soma-soma pairing in 8–10 μg of these RNAi probes. To test for the effectiveness of the RNAi knockdown, total HVA barium currents were measured in whole-cell patch configuration (Fig. 3*B*). RNA interference of *LCa$_v$2* resulted in a dramatic depression of HVA currents, leaving only a residual current with noticeably different inactivation kinetics, which may be due to *LCa$_v$1*, the other HVA channel type identified in VD4. Synaptic transmission was completely abolished with

selective RNAi knockdown of the gene containing the identified short II–III linker (Fig. 3*C*, $n = 7$). As RNAi knockdown was targeted specifically to this LCa_v2 sequence, the absence of a postsynaptic response indicates that neurotransmission relies exclusively on a calcium channel homolog that lacks a *synprint* motif in the II–III linker.

From the experiment shown in Fig. 3*C*, it was unclear whether the lack of synaptic transmission was due to the inability of the VD4 neuron to release neurotransmitter or a consequence of a change in synaptic architecture that prevented the postsynaptic cell from detecting transmitter released from VD4. To discriminate among these possibilities, the dopaminergic neuron RPeD1 was pre-treated with LCa_v2 RNAi as described above. Transmitter release was detected from RPeD1 as a function of non-synaptic electrophysiological responses in a "sniffer" cell (15). After RNAi treatment, RPeD1 somata were plated on poly-L-lysine-coated dishes, and a freshly isolated soma of one of its postsynaptic neurons (visceral K, VK) was manipulated in close proximity to RPeD1 to detect induced release of transmitter. RNAi treatment of RPeD1 rendered this cell incapable of transmitter release (Fig. 3*D*, $n = 13$). In contrast, under control conditions, 100% of RPeD1 cells released dopamine that was detected at some distance by the sniffer cell (Fig. 3*D*, $n = 9$). These data indicate that the loss in synaptic transmission between VD4 and LPeD1 neurons was likely due to a direct effect on neurotransmitter release.

Taken together, the above data indicate that, like in mammalian neurons, Ca_v2 calcium channels are required for transmitter release in *Lymnaea* neurons.

Lymnaea Synaptic Transmission Depends on SNARE Proteins but Not on Their Interactions with the $Lca_2$2 Channels—Previous work (25) in other invertebrate systems suggests that synaptic transmission in *Lymnaea* may also rely on the SNARE proteins syntaxin1A and SNAP-25. As shown in Fig. 4*A*, injection of 1 μM Botulinum toxin (Bt) C1 or BtE into presynaptic VD4 neurons paired with LPeD1 abolished synaptic transmission between these neurons (Fig. 4*A*; $n = 6$ and 5, respectively), without affecting the response of the postsynaptic neuron to exogenously applied ACh, the transmitter used at the VD4-LPeD1 synapse (not shown). Hence, as expected a functional complement of *L*SNAREs in the presynaptic cell is required for transmitter release.

The absence of the *synprint* motif in LCa_v2, however, predicts that *Lymnaea* synaptic proteins such as syntaxin1A, SNAP-25, and synaptotagmin1 should not be able to interact with the II–III linker. Indeed, as shown in Fig. 4, there was no measurable association of the *Lymnaea* II–III linker with GST-*Lstx1A*, GST-*LSNAP25, or* GST-$Lsyt_1$ (Fig. 4*B*) in direct binding assays, whereas comparable amounts of *Lymnaea* synaptic proteins readily bound to the positive control, rat His_6 *synprint* (Fig. 4*B*). We also did not detect binding of these proteins to the LCa_v2 C terminus (Fig. 4*C*), N terminus, domain I–II linker, and domain III–IV linker region *in vitro*, or in a yeast two-hybrid assay (not shown). Moreover, neither the II–III linker nor the C-terminal region bound syntaxin1A in protein extracts of *Lymnaea* whole brain ganglia (Fig. 4*C*), indicating that syntaxin1A is not coupled to these regions of the LCa_v2 channel via adaptor proteins. In contrast, there was consistent, dose-dependent binding of rat *synprint* to *Lymnaea* syntaxin1A from brain extracts (Fig. 4*C*).

Overall, these data indicate that *Lymnaea* orthologs of syntaxin1A, SNAP-25, and synaptotagmin1, although potentially capable of interacting with rat *synprint*, do not associate with the major cytoplasmic regions of the *Lymnaea* homolog of presynaptic calcium channels and thus are unlikely to interact with this channel altogether.

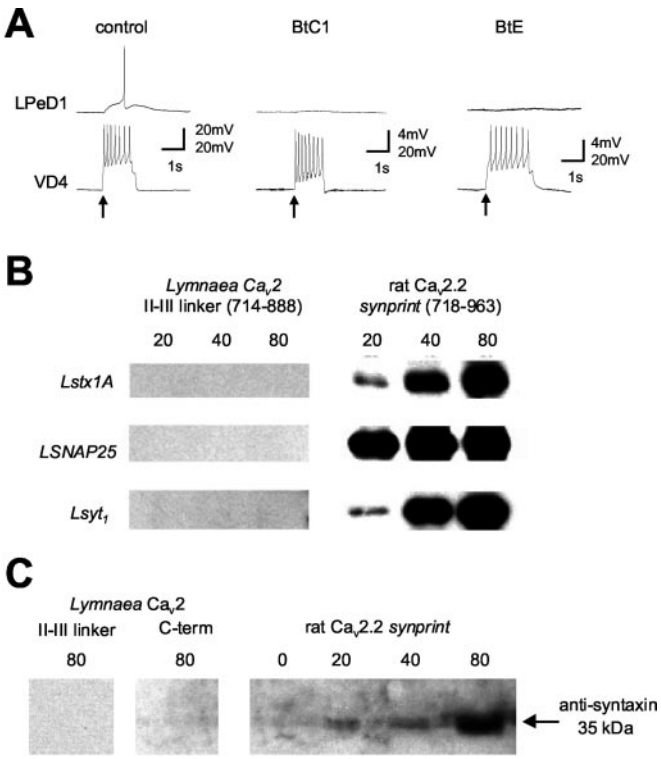

FIG. 4. ***Lymnaea* synaptic transmission depends on SNARE proteins, but not on SNARE protein-calcium channel interactions.** *A*, effect of Botulinum toxins (*Bt*) on synaptic transmission in *Lymnaea*. Unlike in control pairs ($n = 6$), in VD4 neurons injected with BtC1 ($n = 6$) or BtE ($n = 5$), a train of action potentials (*arrow*) in VD4 failed to elicit a postsynaptic response in LPeD1. *B*, *in vitro* binding of His_6-LCa_v2a II–III linker (*left panel*) or the positive control His_6-rat $Ca_v2.2$ *synprint* (*right panel*) to incremental amounts of 20, 40, or 80 μl of a 50% slurry of *Lymnaea* syntaxin1A, SNAP-25, and synaptotagmin1. Western blots were probed with an Anti-Xpress antibody. *C*, *in vitro* experiments involving the binding of 230 μg of *Lymnaea* brain ganglia extracts to immobilized His_6- LCa_v2b II–III linker (80 μl), His_6-LCa_v2a C terminus (80 μl), and His_6-rat $Ca_v2.2$ *synprint* (20, 40 and 80 μl) under identical experimental conditions.

Synprint Peptide Injection into VD4 Perturbs Synaptic Transmission—*Synprint* peptides injected into mammalian SCG neurons disrupt synaptic transmission, perhaps by competitively inhibiting the interaction between syntaxin1A and/or SNAP-25 to N-and P/Q-type channels (7). Because the *Lymnaea* channel ortholog lacks *synprint* and consequently does not appear to associate with these proteins, one would expect that mammalian *synprint* peptide injected into *Lymnaea* VD4 neurons should not affect neurotransmission. Surprisingly, the injection of 8–10 pM of rat *synprint* peptide into VD4 neurons 1–4 h prior to recording interfered with synaptic transmission between VD4-LPeD1 pairs (Fig. 5, $n = 13$). In 7 of 13 *synprint*-injected cells, a complete blockade of transmission was observed. In the remaining synapses a marked use-dependent perturbation of synaptic transmission was noted, such that during a series of 10 action potentials, the postsynaptic response became reduced to 32% of the amplitude of the initial EPSP (Fig. 5, *C* and *D*). These results suggest that the site of *synprint* peptide action was initially inaccessible but became incrementally exposed to *synprint* by repetitive presynaptic stimuli. The presence of the *synprint* peptide *per se* did not affect current densities or the biophysical properties of *Lymnaea* calcium currents (not shown), indicating that the effects of these peptides occurred independently of an action on calcium channels. To ensure that the effects of the *synprint* peptide were specific, we generated a peptide of the domain II–III linker region of the *Lymnaea* Ca_v2 calcium channel which, as

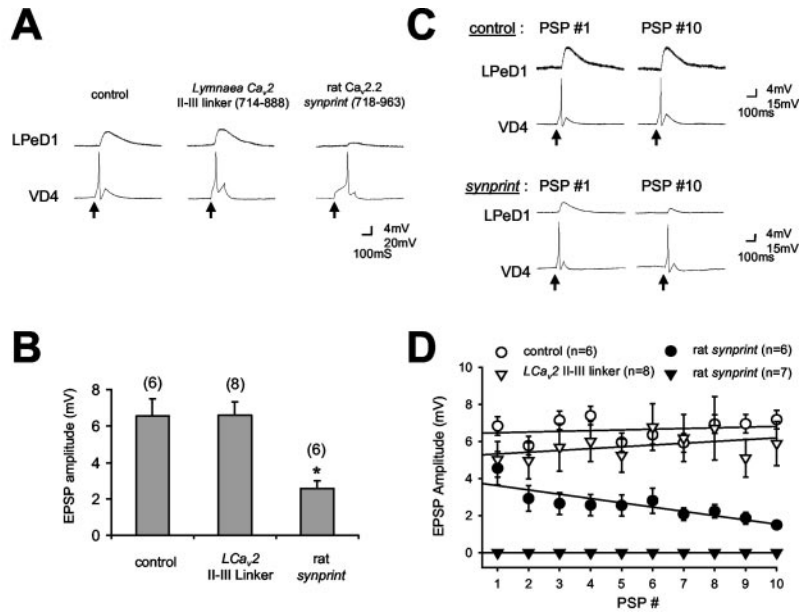

FIG. 5. ***Synprint* peptides prevent *Lymnaea* synaptic transmission.** *A* and *B*, sample recordings (*A*) and bar graph (*B*) (mean EPSP amplitude ± S.D.) representing control pairs or pairs in which the presynaptic VD4 neuron was injected with rat $Ca_v2.2$ *synprint,* or the *Lymnaea* Ca_v2 II–III linker. In ~50% (n = 13) of the *synprint* injected pairs, synaptic transmission is completely abolished (not shown). In the remaining *synprint* injected pairs, the average EPSP amplitude is 2.26 ± 0.40 mV. In control and LCa_v2 II–III linker injected pairs, synaptic transmission was normal. Single action potentials induced in VD4 (*arrow*) elicited 1:1 EPSPs with average amplitude of 6.6 ± 0.96 mV (control, n = 6) and 6.6 ± 0.72 mV (LCa_v2 II–III linker, n = 8). *C* and *D*, the effect of *synprint* displays marked use dependence. In these experiments, all neuron pairs were subjected to a series of 10 action potentials with 30 s between each action potential. Unlike in control cells, or in cells injected with LCa_v2 II–III linker (not shown), in *synprint* injected pairs (*top panel*), the EPSP induced by the 10th action potential is on average 32% smaller than that induced by the 1st action potential. The graph in *D* demonstrates the use-dependent blockade of synaptic transmission in *synprint* injected neurons (*closed circles*). The remaining pairs injected with *synprint* do not display synaptic transmission at any time during our recordings (*closed triangles*). In control (*open circles*) and LCa_v2 II–III linker injected (*open triangles*) pairs, the amplitude of EPSPs remains relatively constant.

shown in Fig. 4*B,* is incapable of interacting with syntaxin 1, SNAP-25, or synaptotagmin. Injection of this peptide into VD4 neurons did not significantly affect synaptic transmission between the paired cells (Fig. 5, *A*, *B*, and *D*). This observation is reminiscent of the inability of rat L-type calcium channel II–III linker peptides to alter synaptic transmission in rat SCG neurons (7), and supports the specificity of the *synprint* peptide effects illustrated in Fig. 5.

Overall, our data suggest that synaptic transmission between *Lymnaea* neurons exhibits many of the hallmarks of mammalian neurotransmission but seems to occur without physical tethering of presynaptic vesicle release complex to a *synprint* region in presynaptic calcium channels. Mammalian *synprint* peptides can nonetheless interfere with neurotransmitter release perhaps by inactivating other synaptic elements that make use of the *synprint* motif.

Alternative Splicing of the Non-L-type Channel Regulates Lymnaea Neurotransmission—As noted above, two splice variants of the LCa_v2 channel with different C-terminal tails are expressed in VD4 neurons (Fig. 2). To determine the significance of this observation for synaptic transmission, we designed a specific RNAi probe against the variant with the extended C terminus, and we assessed its effect on synaptic transmission between VD4 and LPeD1. The selective depletion of the longer C-terminal LCa_v2 variant completely abolished synaptic transmission in 6 of the 9 cells examined, and in the remaining synapses, EPSP amplitude was reduced to 2.1 ± 0.2 mV (see Fig. 6*A*). The loss in synaptic transmission was accompanied by a significant reduction (22.4 ± 3.01 pA/pF, n = 7; p = 0.001 *versus* control) in HVA current densities in RNAi-treated cells (Fig. 6*B*). Although this reduction was substantial, it was nonetheless significantly (p = 0.02) smaller than that seen in Fig. 3*B* which was designed to eliminate all LCa_v2 expression. Indeed, the data shown in Figs. 3*B* and 6*B* are consistent with the observation that the LCa_v2a channel comprises a larger fraction

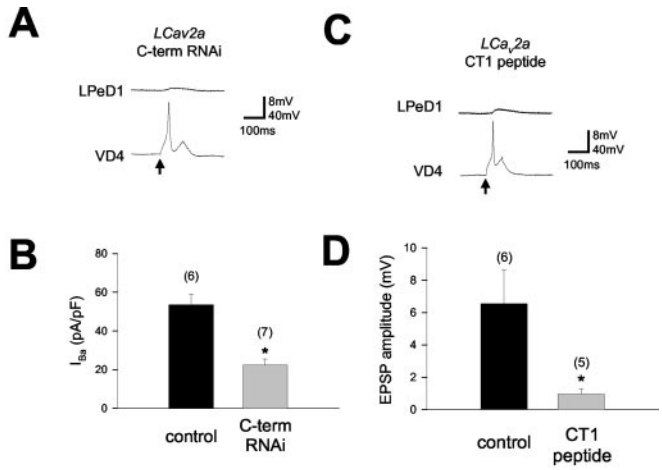

FIG. 6. **Alternative splicing of LCa_v2 is essential for synaptic transmission.** *A*, effect of selective RNAi knockdown of the long form C-terminal splice variant of the LCa_v2 Ca^{2+} channel on EPSPs. The experimental conditions were as outlined in Fig. 3, *B* and *C*, but the RNAi probe was directed against the alternately spliced C-terminal region. Note that in 6 of 9 synapses examined, synaptic transmission was undetectable, whereas in the remaining pairs, EPSP amplitude decreased to about 30% of the control value. *B*, current densities in control cells, and in cells depleted of the LCa_v2 C-terminal splice variant. The control data are the same as those shown in Fig. 3*B*. *C* and *D*, effect of injection of a peptide (*CT1*) corresponding to the alternately spliced C-terminal region in LCa_v2a on synaptic transmission in form of sample traces (*C*) or a bar graph (*D*). Note that this peptide drastically depresses EPSPs in paired VD4/LPeD1 neurons.

of the total LCa_v2 calcium mRNA transcript level (see Fig. 2).

The notion that an alternately spliced C-terminal sequence appears to be essential for synaptic release raises the possibility that this region might be involved in protein-protein interactions at the synapse. To test this possibility, we injected a

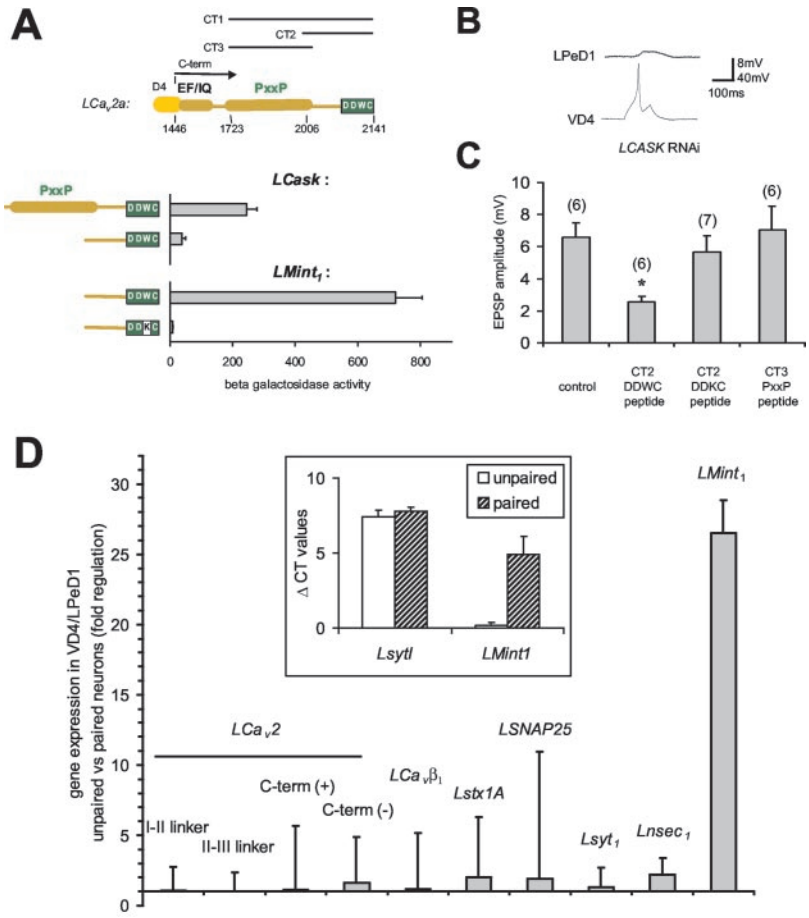

FIG. 7. **Mint1 and CASK regulate *Lymnaea* neurotransmission.** *A*, yeast two-hybrid assay illustrating the binding of Mint1 and CASK to the alternatively spliced C-terminal region of *LCa$_v$2*. Both Mint1 and CASK bind to this region but to separate domains with Mint1 interacting with the extreme C-terminal tail (CT2 region), and CASK binding to an upstream proline-rich region (CT3 region). Site-directed mutagenesis of the tail of the CT2 peptide from DDWC to DDKC abolishes the Mint interaction. Data are expressed in form of β-galactosidase activity determined from liquid extracts. The *top* of the figure depicts a graphic representation of the *LCa$_v$2* channel C-terminal region with the location of CT peptides illustrated above. *B*, sample traces showing that RNAi depletion of VD4 neurons of CASK greatly reduced neurotransmission. In 4 of 7 cells, no EPSPs could be detected, whereas in the remaining cells they were greatly reduced. *C*, effect of injection of CASK interacting CT3 peptides and of wild type and DDKC mutant *LCa$_v$2* CT2 peptides into VD4 neurons on synaptic transmission. Note that the wild type CT2 peptide disrupted neurotransmitter release, whereas the mutant CT2 peptide and the CT3 peptide did not. *D*, qPCR analysis of gene expression of cultured VD4 and LPeD1 neurons, comparing those cultured overnight as VD4/LPeD1 synaptic pairs or unpaired. Whereas the expression of synaptic proteins such as syntaxin1A (*Lstx1A*) and synaptotagmin1 (*Lsyt$_1$*) or calcium channels is not regulated during synapse formation, the expression of *LMint1* is dramatically increased in paired cells. *Inset*, gene expression levels of *Lsyt$_1$* and *LMint1* in unpaired neurons and synaptic pairs. Data are represented as the cycle threshold of detection (*CT*), normalized to the expression of L-*aldolase*. Note the virtual absence of *LMint1* in unpaired neurons. Also note that these experiments differ from those shown in Fig. 2, where only freshly isolated neurons of a single identified type were used for analysis under each condition.

peptide (CT1, see also Fig. 7*A*) directed against this region into VD4 neurons 1 h prior to recording. As shown in Fig. 6, *C* and *D*, this resulted in a dramatic inhibition of synaptic transmission, consistent with the notion that the peptide may have competitively inhibited an interaction between the non-L-type channel C-terminal region and an essential presynaptic protein.

Synaptic Transmission Depends on CASK and Mint1—The alternately spliced C-terminal region in *LCa$_v$2a* contains a proline-rich region with multiple P*XX*P consensus sites for putative association with SH3 domains, as well as a characteristic (D/E)*X*WC motif at the C-terminal, 3′ end (see Figs. 1*D* and 7*A*). Both the (D/E)*X*WC and an upstream proline-rich region are highly conserved in mammalian N- and P/Q-type calcium channels, where they have been shown to bind specifically to the first of two PDZ domains of Mint1 and SH3 domains of CASK, respectively (26–27). To determine whether *LCa$_v$2* C terminus could interact with Mint1 and CASK *in vitro*, we employed a yeast two-hybrid assay, using the *LCa$_v$2a* C terminus as bait and *Lymnaea* Mint1 and CASK as prey. We detected a robust interaction (Fig. 7*A*) with CASK binding to a fragment containing a proline-rich sequence (CT3), whereas Mint1 bound downstream specifically to the C-terminal tail containing DDWC motif (CT2). Mint1 binding was virtually abolished when we introduced a single amino acid mutation W2140K into the CT2 peptide sequence, converting *Lymnaea LCa$_v$2a* DDWC sequence to DDKC, the terminal amino acids reminiscent of rat α_{1E} channels (Fig. 7*A*) (26). Hence, in analogy to what has been reported for rat N-type calcium channels, Mint1 and CASK can bind to the *LCa$_v$2* carboxyl tail, raising the possibility that these interactions might be critically involved in neurotransmission. To test this possibility, we first treated VD4 neurons with RNAi to CASK. This resulted in block of synaptic activity in 4 of 7 experiments and dramatically reduced EPSP amplitude in the remaining cells (Fig. 7*B*), indicating that CASK is essential for synaptic function. Moreover, this is consistent with the possibility that an interaction between CASK and the *LCa$_v$2* C terminus is required to ensure proper neurotransmitter release. There was no detectable change in calcium current density or the biophysical charac-

teristics of the channels after CASK RNAi treatment or in the presence of the C-terminal peptide (not shown), indicating that the observed effects were not due to a change in calcium channel function. We were, however, unable to detect consistent effects of Mint1 RNAi knockdown on synaptic transmission ($n = 25$). This could in principle suggest that Mint1 might not play a key role in synaptic transmission (but see below). Alternatively, it is possible that the knockdown may have been inefficient/incomplete or perhaps that compensation from another Mint isoform could have occurred.

To test further the role of Mint1 and CASK in synaptic transmission, we generated separate peptides corresponding to the CASK and Mint1 binding regions, and we injected them individually into VD4 neurons 1 h prior to recording. Whereas injection of the CASK interacting CT3 peptide did not affect synaptic transmission in 6 of 7 synaptic pairs examined (Fig. 7*C*), the Mint1 interacting CT2 peptide dramatically inhibited synaptic transmission such that 4 of 10 synapses exhibited no detectable transmission, and in the remaining cells EPSP amplitudes were dramatically reduced (Fig. 7*C*). Injection of a DDKC mutant CT2 peptide (which is incapable of binding Mint1, see Fig. 7*A*) resulted in normal EPSPs in 7 of 8 experiments, suggesting that the effects of the Mint1-interacting peptide were indeed specific for the Mint1-calcium channel interaction. Our data are thus consistent with a mechanism in which *Lymnaea* synaptic transmission is dependent on a Mint1-calcium channel interaction, as well as on the presence of CASK.

To determine whether the expression of the calcium channel splice variant and synaptic/scaffolding proteins are dynamically regulated during synaptogenesis, we carried out qPCR analysis of pre- and postsynaptic VD4 and LPeD1 neurons that were either separately cultured or synaptically paired overnight prior to mRNA extraction but were otherwise cultured under identical conditions. As shown in Fig. 7*D*, the expression of the *LCa$_v$2* channel splice variants were not altered during synapse formation, consistent with our previous finding that the development of calcium hotspots during synapse formation appears to involve a redistribution of existing channels (16). Furthermore, there were no obvious gene expression changes observed in SNARE proteins or synaptotagmin1 (see also *inset* to Fig. 7*D*). Interestingly, whereas gene expression of Mint1 was almost undetectable in unpaired neurons (see *inset*), robust Mint1 expression was detected after pairing, indicating that Mint1 may serve as key signaling element during synapse formation. We were unable to perform a similar analysis for CASK, because CASK expression levels were only barely over the detection limit (requiring >36 PCR cycles), thus preventing us from reliably determining changes in CASK expression. Nonetheless, given the profound effects of CASK RNAi knockdown, together with the observations that both Mint1 and CASK bind to specific calcium channel splice variant whose expression is essential for synaptic transmission, suggests that these proteins could regulate synaptic activity via their interaction with calcium channels.

DISCUSSION

Absence of Coupling of SNARE Complexes with Presynaptic Calcium Channels—The *Lymnaea* soma-soma synapse is an emerging model that allows convenient access to identified single pre- and postsynaptic neurons (13, 16). These synapses are morphologically and electrophysiologically similar to those *in vivo* and require new gene transcription and *de novo* protein synthesis to form (13). Moreover, as in mammalian synapses, target cell-specific calcium hotspots develop at the active zones during synapse formation, which appear to result from a redistribution of existing calcium channels rather than the synthesis of new channels (16). Detailed analyses of the molecular players involved in *Lymnaea* synapse formation/function have so far been hampered by a lack of information about the *Lymnaea* genome. We have thus cloned the entire complement of voltage-gated calcium channels, plus a number of key synaptic and scaffolding proteins from *Lymnaea* to provide a novel perspective regarding the relationship between SNARE proteins, calcium channels, and scaffolding proteins during transmitter release at the level of individual pre- and postsynaptic neurons.

Although the SNARE complexes are important for transmitter release from *Lymnaea* neurons, this role appears to be independent of their coupling with calcium channels. Our results therefore contrast with those obtained in vertebrates where a direct association between SNARE complexes and calcium channels was deemed necessary for transmitter release (2, 5). Indeed, the synaptic protein interaction site found in mammalian N-type and P/Q-type calcium channels (4–6) is conspicuously absent in invertebrate Ca$_v$2 orthologs such as in *C. elegans*, *Drosophila* (10), and *Lymnaea*. It has remained unclear as to whether synaptic transmission in invertebrates occurs independently of a calcium channel SNARE protein interaction, or whether invertebrate calcium channels might perhaps harbor a synaptic protein interaction site that is structurally unrelated to that found in mammals (9, 28–31). Because syntaxin1A, SNAP-25, and synaptotagmin1 mainly associate through exposed, cytoplasmic surfaces, any putative synaptic binding domain on the calcium channel would most likely be confined to one of the intracellular loops. Yet, in pull-down assays and/or in yeast two-hybrid assays, we were unable to detect a physical interaction of these proteins with any of the major intracellular regions of the *LCa$_v$2* channel, indicating that they do not directly associate with *LCa$_v$2*. The injection of mammalian *synprint* peptides (but not *LCa$_v$2* II–III linker peptides) nonetheless inhibited synaptic activity without affecting calcium channel function, suggesting that these peptides are capable of non-specifically interfering with synaptic transmission downstream of calcium channels. Alternatively, *synprint* may act as an interaction domain in other as yet unidentified proteins more distantly associated with transmitter release. Our observation of a *synprint* peptide effect in a synapse where calcium channels are apparently uncoupled from SNAREs raises the possibility that similar nonselective effects could have occurred when this peptide was injected into mammalian SCG neurons to uncouple the SNARE complex from voltage-gated calcium channels (2, 7). If so, this would weaken the interpretation that a direct physical coupling between calcium channels and the SNARE complex must be a prerequisite for transmitter release at synapses to ensure proximity of calcium channels to the release sites. The *synprint* region may perhaps serve to optimize the efficiency of synaptic transmission or to serve as a site for regulating calcium channel activity (2, 12, 19, 32–33). Thus, rather than being universally required, the presence of a synaptic protein interaction site in calcium channels may be an evolutionary specialization in the vertebrates.

Possible Role of LCa$_v$2a Channels in Presynaptic Transmitter Release—Despite the absence of a *synprint* motif, calcium hotspots appear to form at the active zones during synapse formation (16). Interestingly, this appears to involve a redistribution of existing calcium channels, rather than the new synthesis of channel protein (16), consistent with our observation that transcript levels of individual calcium channel splice variants did not change during synapse formation. Given that synaptic transmission in *Lymnaea* appears to be critically dependent on the *LCa$_v$2a* channel (*i.e.* the one with the long C terminus that is capable of interacting with Mint1 and CASK),

we propose that interactions between the C terminus and these proteins may be involved in channel clustering at the active zones and perhaps in synaptic transmission *per se*. This would be consistent with the fact that the Mint1 and CASK interaction domains are highly conserved in synaptic calcium channels, and with recent evidence suggesting that synaptic targeting of N-type calcium channels in rat hippocampal neurons is dependent on the C-terminal region of these channels (27).

Although Mint1 and CASK can both interact with the C-terminal region of the channel and have both been implicated in protein targeting functions, they do not appear to have identical cellular functions, with CASK having a role in developmental processes and Mint1 having a closer association with synaptic vesicle exocytosis (34–36). The observations that the expression of Mint1 appeared to occur only following cell-cell contact (see Fig. 7*D*) and that *Lymnaea* synaptic transmission was blocked by injection of Mint1 interacting DDWC-CT2 peptides 1 h prior to recording suggest that the Mint calcium channel interaction may mediate a more acute role in synaptic transmission. In contrast, the CASK interaction may be of greater importance in the earlier stages of synapse formation/channel clustering. This would fit with our observation that injection of the CASK interacting CT3 peptide 1 h prior to recording did not affect synaptic transmission. We also note that the RNAi knockdown of CASK that resulted in the loss of synaptic transmission was initiated prior to synapse formation, again perhaps consistent with an early role of CASK. However, although our data provide evidence for an important role of CASK and the LCa_v2 C-terminal region, we must acknowledge two potential caveats. First, because we did not examine any putative effects of the CT3 peptide during earlier stages of synapse formation, our data do not permit us to determine whether a physical interaction between CASK and the C terminus of the LCa_v2 channel is indeed of physiological significance. Second, although a single point mutation in the CT2 peptide prevented both Mint1 binding and, in parallel, abolished the physiological effects of this peptide, we cannot rule out the possibility that another protein recognizing the Mint1-binding site on the LCa_v2 calcium channel could be antagonized by the CT2 peptide. Our experimental data at this stage do not allow us to firmly implicate Mint1 in synaptic transmission. Further experiments will therefore be needed to prove a role of Mint1 in synaptic transmission, and to define the temporal sequence of the involvement of CASK (and possibly Mint1) in synapse formation and synaptic activity.

Taken together, it appears that an interaction of presynaptic calcium channels with scaffolding proteins appears to be more fundamental for synaptic transmission than direct coupling to syntaxin, SNAP-25 and synaptotagmin. This may have implications for understanding the roles of other types of presynaptic calcium channels that lack the *synprint* motif, such as certain splice variants of the human N-type channel (37) and apparently all types of non-vertebrate calcium channels identified to date. Such differences likely contribute to the observed synaptic diversity across cell types and species (38).

REFERENCES

1. Neher, E. (1998) *Neuron* **20,** 389–399
2. Rettig, J., Heinemann, C., Ashery, U., Sheng, Z. H., Yokoyama, C. T., Catterall, W. A., and Neher, E. (1997) *J. Neurosci.* **17,** 6647–6656
3. Stanley, E. F. (1997) *Trends Neurosci.* **20,** 404–409
4. Sheng, Z. H., Rettig, J., Takahashi, M., and Catterall, W. A. (1994) *Neuron* **13,** 1303–1313
5. Sheng, Z. H., Rettig, J., Cook, T., and Catterall, W. A. (1996) *Nature* **379,** 451–454
6. Sheng, Z. H., Yokoyama, C. T., and Catterall, W. A. (1997) *Proc. Natl. Acad. Sci. U. S. A.* **94,** 5405–5410
7. Mochida, S., Sheng, Z. H., Baker, C., Kobayashi, H., and Catterall, W. A. (1996) *Neuron* **17,** 781–788
8. Mochida, S., Yokoyama, C. T., Kim, D. K., Itoh, K., and Catterall, W. A. (1998) *Proc. Natl. Acad. Sci. U. S. A.* **95,** 14523–14528
9. Lloyd, T. E., Verstreken, P., Ostrin, E. J., Phillippi, A., Lichtarge, O., and Bellen, H. J. (2000) *Neuron* **26,** 45–50
10. Littleton, J. T., and Ganetzky, B. (2000) *Neuron* **26,** 35–43
11. Jarvis, S. E., Magga, J. M., Beedle, A. M., Braun, J. E., and Zamponi, G. W. (2000) *J. Biol. Chem.* **275,** 6388–6394
12. Jarvis, S. E., and Zamponi, G. W. (2001) *Trends Pharmacol. Sci.* **22,** 519–525
13. Feng, Z. P., Klumperman, J., Lukowiak, K., and Syed, N. I. (1997) *J. Neurosci.* **17,** 7839–7849
14. van Kesteren, R. E., Syed, N. I., Munno, D. W., Bouwman, J., Feng, Z. P., Geraerts, W. P., and Smit, A. B. (2001) *J. Neurosci.* **21,** RC161
15. Spencer, G. E., Lukowiak, K., and Syed, N. I. (2000) *J. Neurosci.* **20,** 8077–8086
16. Feng, Z. P., Grigoriev, N., Munno, D., Lukowiak, K., MacVicar, B. A., Goldberg, J. I., and Syed, N. I. (2002) *J. Physiol.* (*Lond.*) **539,** 53–65
17. Lee, J. H., Cribbs, L. L., and Perez-Reyes, E. (1999) *FEBS Lett.* **445,** 231–236
18. Takahashi, T., and Momiyama, A. (1993) *Nature* **366,** 156–158
19. Jarvis, S. E., and Zamponi, G. W. (2001) *J. Neurosci.* **21,** 2939–2948
20. Kawasaki, F., Felling, R., and Ordway, R. W. (2000) *J. Neurosci.* **20,** 4885–4889
21. Smith, L. A., Wang, X., Peixoto, A. A., Neumann, E. K., Hall, L. M., and Hall, J. C. (1996) *J. Neurosci.* **16,** 7868–7879
22. Schafer, W. R., and Kenyon, C. J. (1995) *Nature* **375,** 73–78
23. Pragnell, M., De Waard, M., Mori, Y., Tanabe, T., Snutch, T. P., and Campbell, K. P. (1994) *Nature* **368,** 67–70
24. Smit, A. B., Syed, N. I., Schaap, D., van Minnen, J., Klumperman, J., Kits, K. S., Lodder, H., van der Schors, R. C., van Elk, R., Sorgedrager, B., Brejc, K., Sixma, T. K., and Geraerts, W. P. (2001) *Nature* **411,** 261–268
25. O'Connor, V., Heuss, C., De Bello, W. M., Dresbach, T., Charlton, M. P. Hunt, J. H., Pellegrini, L. L., Hodel, A., Burger, M. M., Betz, H., Augustine, G. J., and Schafer, T. (1997) *Proc. Natl. Acad. Sci. U. S. A.* **94,** 12186–12191
26. Maximov, A., Sudhof, T. C., and Bezprozvanny, I. (1999) *J. Biol. Chem.* **274,** 24453–24456
27. Maximov, A., and Bezprozvanny, I. (2002) *J. Neurosci.* **22,** 6939–6952
28. Wu, M. N., Fergestad, T., Lloyd, T. E., He, Y., Broadie, K., and Bellen, H. J. (1999) *Neuron* **23,** 593–605
29. Fergestad, T., Wu, M. N., Schulze, K. L., Lloyd, T. E., Bellen, H. J., and Broadie, K. (2001) *J. Neurosci.* **21,** 9142–9150
30. Littleton, J. T., Chapman, E. R., Kreber, R., Garment, M. B., and Carlson, S. D., and Ganetzky, B. (1998) *Neuron* **21,** 401–413
31. Littleton, J. T., Serano, T. L., Rubin, G. M., Ganetzky, B., and Chapman, E. R. (1999) *Nature* **400,** 757–760
32. Bezprozvanny, I., Scheller, R. H., and Tsien, R. W. (1995) *Nature* **378,** 623–626
33. Magga, J. M., Jarvis, S. E., Arnot, M. I., Zamponi, G. W., and Braun, J. E. (2000) *Neuron* **28,** 195–204
34. Laverty, H. G., and Wilson, J. B. (1998) *Genomics* **53,** 29–41
35. Okamoto, M., and Sudhof, T. C. (1997) *J. Biol. Chem.* **272,** 31459–31464
36. Tabuchi, K., Biederer, T., Butz, S., and Sudhof, T. C. (2002) *J. Neurosci.* **22,** 4264–4273
37. Kaneko, S., Cooper, C. B., Nishioka, N., Yamasaki, H., Suzuki, A., Jarvis, S. E., Akaike, A., Satoh, M., and Zamponi, G. W. (2002) *J. Neurosci.* **22,** 82–92
38. Atwood, H. L., and Karunanithi, S. (2002) *Nat. Rev. Neurosci.* **3,** 497–516